

Maximum Likelihood Estimation in Data-Driven Modeling and Control

Mingzhou Yin, Andrea Iannelli, and Roy S. Smith, *Fellow, IEEE*

Abstract—Recently, various algorithms for data-driven simulation and control have been proposed based on the Willems’ fundamental lemma. However, when collected data are noisy, these methods lead to ill-conditioned data-driven model structures. In this work, we present a maximum likelihood framework to obtain an optimal data-driven model, the signal matrix model, in the presence of output noise. A data compression scheme is also proposed to enable more efficient use of large datasets. Two approaches in system identification and receding horizon control are developed based on the derived optimal estimator. The first one identifies a finite impulse response model in combination with the kernel-based method. This approach improves the least-squares-based estimator with less restrictive assumptions. The second one applies the signal matrix model as the predictor in predictive control. The control performance is shown to be better than existing data-driven predictive control algorithms, especially under high noise levels. Both approaches demonstrate that the derived estimator provides a promising framework to apply data-driven algorithms to noisy data.

Index Terms—Data-driven modeling, maximum likelihood estimation, model predictive control, system identification.

I. INTRODUCTION

FOLLOWING its remarkable success in artificial intelligence, learning from data is becoming a popular topic in various engineering domains [1]. This concept is by no means a new idea for control engineering. The system identification paradigm has been widely used in control applications, where data are used to fit an a priori parametrized model structure [2]. The control strategy is then designed with the identified nominal model based on the certainty equivalence principle [3], or with the uncertainty model based on robust/stochastic control frameworks, possibly with adaptive elements also learned from online data [4].

However, this conventional scheme of learning dynamical systems is challenged by increasing complexity of systems and the large amount of data available. In particular, a low-dimensional model structure that is suitable to design compact, closed-form control strategies can be very hard and costly to obtain for complex systems [5]. In fact, low dimensionality

is not really required in modern optimization-based control frameworks, and may limit the predictive power of big data [6]. Therefore, alternative paths are investigated to facilitate control design directly from raw measurement data from dynamical systems. Early attempts in this direction include unfalsified control [7], iterative feedback tuning [8], and virtual reference feedback tuning [9]. Reinforcement learning techniques are also widely pursued in this area [10], including policy search [11] and approximate dynamic programming [12].

The above approaches typically avoid predicting the behavior of systems explicitly but aim at the control strategy directly. On the other hand, it is possible to directly replace the conventional model with a data-driven predictor [13]. In the seminal work from Willems *et al.* [14], a single input-output trajectory of the linear system is shown to be able to characterize all possible trajectories of length up to the order of persistency of excitation by constructing Hankel matrices from data. This result is known as the Willems’ fundamental lemma. With this result, the behavior of the system can be simulated and thus controlled by selecting a suitable combination of sections from the known trajectory that satisfies the initial condition constraints [15]–[17].

This observation is especially suitable for optimal trajectory tracking. In this regard, model predictive control (MPC) is known to be very effective when an accurate model of the system is available [18]. From the Willems’ fundamental lemma, the future output prediction step in MPC can be achieved by using known trajectories of the system directly, instead of an explicit model. This data-driven alternative to MPC algorithms, known as data-enabled predictive control (DeePC) [19], has led to multiple successful applications [20]–[22] with a recent stability and robustness proof [23].

Although this data-driven approach is often promoted as model-free, it effectively provides a model of system trajectory based on known data. With a low-rank approximation, this approach directly leads to the intersection algorithm in subspace identification where state-space models can be derived [24]. The main differences of the data-driven approach compared to the conventional model-based methods are: 1) the model is implicit and as such there is no closed-form solution of the model in general; 2) the model is over-parametrized in that it does not impose any assumption on the system structure other than linearity. In this paper, this implicit and over-parametrized model is called the data-driven model.

However, it is well-known that when data are noisy, over-parametrized models may lead to high variances and overfitting [25]. In data-driven modeling, finding a combination of known trajectory sections that give reliable prediction is an ill-

This work was supported by the Swiss National Science Foundation under Grant 200021.178890.

This work has been submitted to the IEEE for possible publication. Copyright may be transferred without notice, after which this version may no longer be accessible.

The authors are with the Automatic Control Laboratory, Swiss Federal Institute of Technology (ETH Zürich), 8092 Zurich, Switzerland (e-mail: myin@control.ee.ethz.ch; iannelli@control.ee.ethz.ch; rsmith@control.ee.ethz.ch).

conditioned problem for datasets with stochastic noise. In current data-driven control schemes empirical regularizers [19], [23] or least-norm problems [20], [26], [27] are introduced to select a reasonable combination for prediction. Yet, it is not clear what is the optimal way to combine a large set of known trajectory sections to achieve the most reliable prediction. In addition, the hyperparameters in the empirical regularizers are difficult to tune.

Another application of data-driven modeling is to simulate the system response [28], [29]. The main advantage of applying this approach in system identification is that it gives the correct estimation of nonparametric models in the noise-free case. Again in this scenario, the best practice for solving the underdetermined linear system in the Willems' fundamental lemma in the noisy case is not understood. For computational simplicity, the Moore-Penrose pseudoinverse solution that solves the least-norm problem is often the default choice [20], leading to the data-driven subspace predictor [27].

As can be seen from the above discussion, one of the central questions in data-driven approaches based on the Willems' fundamental lemma is how to obtain the optimal data-driven model from a large noise-corrupted dataset [30]. Therefore, in the first part of the paper, we propose a maximum likelihood estimation (MLE) framework to estimate such an optimal model with noise in both offline data and online measurements. This optimal model is named the signal matrix model (SMM). This framework optimizes the combination of offline trajectories by maximizing the conditional probability of observing the predicted output trajectory and the measured past outputs. In addition, a preconditioning strategy is proposed based on singular value decomposition (SVD) to compress the data matrix such that the complexity of the algorithm is only dependent on the trajectory length to be simulated, to the benefit of large datasets.

In the second part of the paper, we present two scenarios where the SMM leads to effective algorithms: 1) estimating finite impulse response (FIR) models with the kernel-based method in system identification; and 2) obtaining a tuning-free data-driven predictive control scheme. In the first scenario, the kernel-based method is used to derive a maximum a posteriori (MAP) estimator based on the impulse response estimate learned from data. Carefully designed kernels encode appropriate characteristics of the dynamical system. Conventionally, the data-based estimate is obtained by least-squares regression. In this work, it is replaced by the signal matrix model simulated with an impulse, which guarantees that an unbiased estimate is obtained. Results show that the model fitting is enhanced when the transient response is unknown or the truncation error of the impulse response is large.

In the second scenario, we replace the prediction part in the DeePC algorithm with the SMM. This predictor is shown to be superior to the pseudoinverse subspace predictor in predictive control. The main advantage of the proposed algorithm is that it avoids the difficult hyperparameter tuning problem in regularized DeePC. The control performance of the proposed algorithm is shown to be better than the DeePC algorithm with optimal hyperparameters when the noise is significant, and similar in the low noise scenario.

The remainder of the paper is organized as follows. Section II defines the notions and preliminaries used in the paper. Section III reviews the Willems' fundamental lemma for finite-dimensional systems and its application to deterministic systems. Section IV derives the signal matrix model with MLE and presents an optimal data-driven simulation algorithm with a data compression scheme. This model is then applied to two problems: Section V identifies an FIR model using SMM simulation and the kernel-based regularization; Section VI applies the SMM predictor in predictive control. Section VII concludes the paper.

II. NOTATION & PRELIMINARIES

For a vector x , the weighted l_2 -norm $(x^\top P x)^{\frac{1}{2}}$ is denoted by $\|x\|_P$. The symbol $\mathcal{N}(\mu, \Sigma)$ indicates a Gaussian distribution with mean μ and covariance Σ . The expectation and the covariance of a random vector x are denoted by $\mathbb{E}(x)$ and $\text{cov}(x)$ respectively. For a matrix X , the vectorization operator stacks its columns in a single vector and is denoted by $\text{vec}(X)$; X^\dagger indicates the Moore-Penrose pseudoinverse; $(X)_{i,j}$ denotes the (i, j) -th entry of X . The symbol \mathbb{S}_{++}^n indicates the set of n -by- n positive definite matrix. For a sequence of matrices X_1, \dots, X_n , we denote $[X_1^\top \dots X_n^\top]^\top$ by $\text{col}(X_1, \dots, X_n)$. Given a signal $x: \mathbb{Z} \rightarrow \mathbb{R}^n$, its trajectory from k to $k+N-1$ is denoted as $(x_i)_{i=k}^{k+N-1}$, and in the vector form as $\mathbf{x} = \text{col}(x_k, \dots, x_{k+N-1})$.

Consider a discrete-time linear time-invariant (LTI) system with output noise, given by

$$\begin{cases} x_{t+1} &= Ax_t + Bu_t, \\ y_t &= Cx_t + Du_t + w_t, \end{cases} \quad (1)$$

where $x_t \in \mathbb{R}^{n_x}$, $u_t \in \mathbb{R}^{n_u}$, $y_t \in \mathbb{R}^{n_y}$, $w_t \in \mathbb{R}^{n_w}$ are the states, inputs, outputs, and output noise respectively. The system is denoted compactly by (A, B, C, D) . The pair (A, B) is controllable if $[B \ AB \ \dots \ A^{n_x-1}B]$ has full row rank; the pair (A, C) is observable if $\text{col}(C, CA, \dots, CA^{n_x-1})$ has full column rank. The system is minimal if (A, B) is controllable and (A, C) is observable.

The notion of persistency of excitation is defined as follows.

Definition 1: A signal trajectory $(x_i)_{i=0}^{N-1} \in \mathbb{R}^n \times \{0, \dots, N-1\}$ is said to be persistently exciting of order L if the block Hankel matrix

$$X = \begin{bmatrix} x_0 & x_1 & \cdots & x_{M-1} \\ x_1 & x_2 & \cdots & x_M \\ \vdots & \vdots & \ddots & \vdots \\ x_{L-1} & x_L & \cdots & x_{N-1} \end{bmatrix} \in \mathbb{R}^{Ln \times M} \quad (2)$$

has full row rank, where $M = N - L + 1$ [14].

Intuitively, this definition means that sections of length L of the trajectory span \mathbb{R}^{Ln} . When used as the input to a linear dynamical system, it can thus excite all the possible behaviors of the system in a window of length L . A necessary condition of Definition 1 is $N \geq L(n+1) - 1$, which gives a lower bound on the trajectory length.

III. DATA-DRIVEN MODELING FOR FINITE-DIMENSIONAL SYSTEMS

In this section, we first review the Willems' fundamental lemma and a few related results in a state-space formulation, followed by an overview of deterministic data-driven simulation and control.

A. Willems' Fundamental Lemma

Built on the notion of the persistency of excitation, the Willems' fundamental lemma shows that all the behavior of a linear system can be captured by a single persistently exciting trajectory of the system when no noise is present. This lemma was originally proposed in the context of behavioral system theory [14], [31], where systems are characterized by the subspace that contains all possible trajectories. It was later reformulated in the state-space context [16], [17]. In the state-space formulation, the output trajectory is unique to a particular input trajectory when a past sufficiently exciting input-output trajectory is specified as the initial condition. The length of the past trajectory should not be shorter than the state dimension. This idea has strong ties with the intersection algorithm in subspace identification [24], where a low-order subspace of the data matrices that corresponds to a low state dimension is sought.

We summarize the available results on data-driven modeling based on the Willems' fundamental lemma for finite-dimensional LTI systems, which are the foundation for the data-driven methods discussed in this paper. These results hold exactly only when the system is noise-free, i.e., $\forall i, w_i = 0$.

Theorem 1: Consider a finite-dimensional LTI system (A, B, C, D) . Let $(u_i^d, x_i^d, y_i^d)_{i=0}^{N-1}$ be a triple of input-state-output trajectory of the system. If the pair (A, B) is controllable and the input is persistently exciting of order $(L + n_x)$, then

(a) the matrix

$$\begin{bmatrix} X \\ U \end{bmatrix} := \begin{bmatrix} x_0^d & x_1^d & \cdots & x_{M-1}^d \\ u_0^d & u_1^d & \cdots & u_{M-1}^d \\ \vdots & \vdots & \ddots & \vdots \\ u_{L-1}^d & u_L^d & \cdots & u_{N-1}^d \end{bmatrix} \quad (3)$$

has full row rank (Corollary 2 in [14], Theorem 1(i) in [17], Lemma 1 in [16]);

(b) the pair $(u_i, y_i)_{i=0}^{L-1}$ is an input-output trajectory of the system iff there exists g , such that

$$\begin{bmatrix} u_0 \\ \vdots \\ u_{L-1} \\ y_0 \\ \vdots \\ y_{L-1} \end{bmatrix} = \begin{bmatrix} U \\ Y \end{bmatrix} g := \begin{bmatrix} u_0^d & u_1^d & \cdots & u_{M-1}^d \\ \vdots & \vdots & \ddots & \vdots \\ u_{L-1}^d & u_L^d & \cdots & u_{N-1}^d \\ y_0^d & y_1^d & \cdots & y_{M-1}^d \\ \vdots & \vdots & \ddots & \vdots \\ y_{L-1}^d & y_L^d & \cdots & y_{N-1}^d \end{bmatrix} g \quad (4)$$

(Theorem 1 in [14], Theorem 1(ii) in [17], Lemma 2 in [16]);

(c) $\text{rank} \left(\begin{bmatrix} U \\ Y \end{bmatrix} \right) = n_x + n_u L$ (Theorem 2 in [24]).

Furthermore, if the system is minimal,

- (d) the immediate past input-output trajectory $(u_i, y_i)_{i=-L_0}^{-1}$ uniquely determines the initial condition x_0 , if $L_0 \geq n_x$ (Lemma 1 in [15]);
- (e) let $L' = L - L_0$, then $(y_i)_{i=0}^{L'-1}$ is the unique output trajectory of the system with past trajectory $(u_i, y_i)_{i=-L_0}^{-1}$ and input trajectory $(u_i)_{i=0}^{L'-1}$, iff there exists g , such that

$$\begin{bmatrix} u_{-L_0} \\ \vdots \\ u_{L'-1} \\ y_{-L_0} \\ \vdots \\ y_{L'-1} \end{bmatrix} = \begin{bmatrix} U \\ Y \end{bmatrix} g := \begin{bmatrix} u_0^d & u_1^d & \cdots & u_{M-1}^d \\ \vdots & \vdots & \ddots & \vdots \\ u_{L'-1}^d & u_L^d & \cdots & u_{N-1}^d \\ y_0^d & y_1^d & \cdots & y_{M-1}^d \\ \vdots & \vdots & \ddots & \vdots \\ y_{L'-1}^d & y_L^d & \cdots & y_{N-1}^d \end{bmatrix} g \quad (5)$$

(Proposition 1 in [15]).

In Theorem 1, parts (a) and (b) state the original Willems' fundamental lemma; part (c) draws the connection between data-driven modeling and subspace identification methods; and parts (d) and (e) further give the uniqueness of the trajectory by fixing a sufficiently long past trajectory. Parts (d) and (e) allow the formulation to be applied in simulation and predictive control.

B. Deterministic Data-Driven Simulation and Control

In the noise-free case, the system can be simulated solely based on a known trajectory by applying Theorem 1(e) [28]. Define

$$U_p = \begin{bmatrix} u_0^d & u_1^d & \cdots & u_{M-1}^d \\ \vdots & \vdots & \ddots & \vdots \\ u_{L_0-1}^d & u_{L_0}^d & \cdots & u_{M+L_0-2}^d \end{bmatrix} \in \mathbb{R}^{L_0 n_u \times M}, \quad (6)$$

$$U_f = \begin{bmatrix} u_{L_0}^d & u_{L_0+1}^d & \cdots & u_{M+L_0-1}^d \\ \vdots & \vdots & \ddots & \vdots \\ u_{L-1}^d & u_L^d & \cdots & u_{N-1}^d \end{bmatrix} \in \mathbb{R}^{L' n_u \times M}, \quad (7)$$

$$\mathbf{u}_{\text{ini}} = \begin{bmatrix} u_{-L_0} \\ \vdots \\ u_{-1} \end{bmatrix} \in \mathbb{R}^{L_0 n_u}, \quad \mathbf{u} = \begin{bmatrix} u_0 \\ \vdots \\ u_{L'-1} \end{bmatrix} \in \mathbb{R}^{L' n_u}, \quad (8)$$

and similarly for $Y_p, Y_f, \mathbf{y}_{\text{ini}}$, and \mathbf{y} . Then we interpret (5) as an implicit model of the system trajectory parametrized by g , namely

$$\begin{cases} \mathbf{u} = U_f g, \\ \mathbf{y} = Y_f g, \end{cases} \quad (9a) \quad (9b)$$

subject to the initial condition requirement

$$\begin{cases} \mathbf{u}_{\text{ini}} = U_p g, \\ \mathbf{y}_{\text{ini}} = Y_p g. \end{cases} \quad (10a) \quad (10b)$$

Thus, the system can be simulated by means of a two-step approach with g as the intermediate parameter as shown in Algorithm 1. The system identification process is performed online for a particular input by estimating g . This algorithm

effectively gives an implicit model of the system in the form of

$$\mathbf{y} = f(\mathbf{u}; \mathbf{u}_{\text{ini}}, \mathbf{y}_{\text{ini}}, U_p, U_f, Y_p, Y_f), \quad (11)$$

where U_p, U_f, Y_p, Y_f are offline data that describe the behaviors of the system, and $\mathbf{u}_{\text{ini}}, \mathbf{y}_{\text{ini}}$ are online data that estimate the initial condition.

Algorithm 1 Noise-free data-driven simulation [28]

- 1: **Given:** U_p, U_f, Y_p, Y_f .
- 2: **Input:** $\mathbf{u}_{\text{ini}}, \mathbf{y}_{\text{ini}}, \mathbf{u}$.
- 3: Solve the linear system

$$\begin{bmatrix} \mathbf{u}_{\text{ini}} \\ \mathbf{y}_{\text{ini}} \\ \mathbf{u} \end{bmatrix} = \begin{bmatrix} U_p \\ Y_p \\ U_f \end{bmatrix} g \quad (12)$$

for g .

- 4: **Output:** $\mathbf{y} = Y_f g$.
-

Multiple control algorithms have been developed based on this model structure [15], [16]. In this work, we focus on the optimal trajectory tracking problem, which optimizes the following control cost over a horizon of length L' at each time instant t [18]:

$$J_{\text{ctr}}(\mathbf{u}, \mathbf{y}) = \sum_{k=0}^{L'-1} \left(\|y_k - r_{t+k}\|_Q^2 + \|u_k\|_R^2 \right), \quad (13)$$

where \mathbf{r} is the reference trajectory, and Q and R are the output and the input cost matrices respectively [18]. At each time instant, the first entry in the newly optimized input trajectory is applied to the system in a receding horizon fashion.

Algorithm 1 can be applied as the predictor in place of the model-based predictor in conventional MPC algorithms. This leads to the following optimization problem

$$\begin{aligned} & \underset{\mathbf{u}, \mathbf{y}, g}{\text{minimize}} && J_{\text{ctr}}(\mathbf{u}, \mathbf{y}) \\ & \text{subject to} && (9), (10), \mathbf{u} \in \mathcal{U}, \mathbf{y} \in \mathcal{Y}, \end{aligned} \quad (14)$$

where \mathcal{U} and \mathcal{Y} are the constraint sets of the inputs and the outputs respectively. Vectors \mathbf{u}_{ini} and \mathbf{y}_{ini} are the immediate past input-output measurements online. This method is known as the unregularized DeePC algorithm [19].

IV. MAXIMUM LIKELIHOOD DATA-DRIVEN MODEL: SIGNAL MATRIX MODEL

The linear system (12) is highly underdetermined when a large dataset is available. When the data are noise-free, this parameter estimation problem is trivial, where any solution to (12) gives an exact output model of the system, according to Theorem 1(e).

However, the problem of finding the model (11) becomes ill-conditioned when the data are noisy. In this case, Theorem 1(c) is no longer satisfied. Instead, $\text{col}(U, Y)$ has full row rank almost surely. If we still follow Algorithm 1, any output trajectory \mathbf{y} can be obtained by choosing different solutions to (12). In fact, Theorem 1(e) does not hold exactly for the noisy case, so satisfying condition (12) is not guaranteed to be

statistically optimal. An empirical remedy to this problem is to use the Moore-Penrose pseudoinverse solution of g , namely

$$g_{\text{pinv}} = \begin{bmatrix} U_p \\ Y_p \\ U_f \end{bmatrix}^\dagger \begin{bmatrix} \mathbf{u}_{\text{ini}} \\ \mathbf{y}_{\text{ini}} \\ \mathbf{u} \end{bmatrix}, \quad (15)$$

which solves the least-norm problem

$$\begin{aligned} & \underset{g}{\text{minimize}} && \|g\|_2^2 \\ & \text{subject to} && (12). \end{aligned} \quad (16)$$

This solution is known as the subspace predictor related to the prediction error method [20], [27]. However, this predictor fails to appropriately encode the effects of noise in the data matrices. To the best of our knowledge, there is no existing statistical framework for estimating g . In what follows, we will derive a maximum likelihood estimator of g . As opposed to existing algorithms, this estimator obtains a statistically optimal data-driven model for systems with noise. Since this model is expressed purely in terms of matrices of signal trajectories, we name this model the signal matrix model. For simplicity of exposition, the results in the section are stated for the single-input single-output case, but they seamlessly hold for the multiple-input multiple-output case.

A. Derivation of the Maximum Likelihood Estimator

In this work, we consider a scenario where the output errors are i.i.d. Gaussian noise for both offline data and online data, i.e.,

$$y_i^d = y_i^{d,0} + w_i^d, \quad (w_i^d)_{i=0}^{N-1} \sim \mathcal{N}(0, \sigma^2 \mathbb{I}), \quad (17)$$

$$\mathbf{y}_{\text{ini}} = \mathbf{y}_{\text{ini}}^0 + \mathbf{w}_p, \quad \mathbf{w}_p \sim \mathcal{N}(0, \sigma_p^2 \mathbb{I}). \quad (18)$$

Remark 1: The formulation can be extended to other noise models in a straightforward way, including correlated noise, input noise, and alternative noise distributions. For example, when the noise is Laplacian, it would lead to an l_1 -norm penalization in the estimator similar to the regularizer proposed in [19].

Under this noise model, the equations (9a) and (10a) still hold exactly, but the past output equation (10b) includes noise on both sides, which leads to a total least squares problem. In this work, the maximum likelihood interpretation of the total least squares problem is used [32].

Define

$$\hat{\mathbf{y}} = \begin{bmatrix} \epsilon_y \\ \mathbf{y} \end{bmatrix} = Yg - \begin{bmatrix} \mathbf{y}_{\text{ini}} \\ \mathbf{0} \end{bmatrix}, \quad (19)$$

where $\epsilon_y := Y_p g - \mathbf{y}_{\text{ini}}$ is the residual of the past output relation (10b). Then we want to construct an estimator that maximizes the conditional probability of observing the realization $\hat{\mathbf{y}}$ corresponding to the available data given g . Applying vectorization on Yg in (19), we have

$$\hat{\mathbf{y}} = (g^T \otimes \mathbb{I}) \text{vec}(Y) - \begin{bmatrix} \mathbf{y}_{\text{ini}} \\ \mathbf{0} \end{bmatrix}, \quad (20)$$

where we make use of the property of the Kronecker product

$$\text{vec}(ABC) = (C^T \otimes A) \text{vec}(B). \quad (21)$$

Denote the noise-free version of Y_p and Y_f by Y_p^0 and Y_f^0 respectively. Then for a given g , we have

$$\begin{aligned}\mathbb{E}(\hat{y}|g) &= \mathbb{E}(Y)g - \begin{bmatrix} \mathbb{E}(\mathbf{y}_{\text{ini}}) \\ \mathbf{0} \end{bmatrix} = \begin{bmatrix} Y_p^0 g - \mathbf{y}_{\text{ini}}^0 \\ Y_f^0 g \end{bmatrix} = \begin{bmatrix} \mathbf{0} \\ Y_f^0 g \end{bmatrix}, \\ \text{cov}(\hat{y}|g) &= (g^\top \otimes \mathbb{I}) \Sigma_{yd} (g \otimes \mathbb{I}) + \begin{bmatrix} \sigma^2 \mathbb{I} & \mathbf{0} \\ \mathbf{0} & \mathbf{0} \end{bmatrix} =: \Sigma_y,\end{aligned}\quad (22)$$

where $\Sigma_{yd} = \text{cov}(\text{vec}(Y))$. According to the noise model of (y_i^d) and accounting for the Hankel structure of Y , we have

$$(\Sigma_{yd})_{i,j} = \begin{cases} \sigma^2, & (\text{vec}(Y))_i = (\text{vec}(Y))_j \\ 0, & \text{otherwise} \end{cases}. \quad (23)$$

Then, Σ_y can be calculated as

$$(\Sigma_y)_{i,j} = \sigma^2 \sum_{k=1}^{M-|i-j|} g_k g_{k+|i-j|} + \begin{cases} \sigma_p^2, & i = j \leq L_0 \\ 0, & \text{otherwise} \end{cases}. \quad (24)$$

where g_k denotes the k -th entry of g . The derivation is given in Appendix I. Thus, due to the linearity of the normal distribution, we have

$$\hat{y}|g \sim \mathcal{N} \left(\begin{bmatrix} \mathbf{0} \\ Y_f^0 g \end{bmatrix}, \Sigma_y \right), \quad (25)$$

which has the distribution

$$\begin{aligned}p(\hat{y}|g) &= (2\pi)^{-\frac{L}{2}} \det(\Sigma_y)^{-\frac{1}{2}} \\ &\exp \left(-\frac{1}{2} \begin{bmatrix} Y_p g - \mathbf{y}_{\text{ini}} \\ Y_f g - Y_f^0 g \end{bmatrix}^\top \Sigma_y^{-1} \begin{bmatrix} Y_p g - \mathbf{y}_{\text{ini}} \\ Y_f g - Y_f^0 g \end{bmatrix} \right).\end{aligned}\quad (26)$$

Note that here the true output data matrix Y_f^0 is also unknown, and can be estimated with the maximum likelihood approach. In this way, we are ready to derive the signal matrix model by solving the following optimization problem.

$$\underset{g \in \mathcal{G}, Y_f^0}{\text{minimize}} \quad -\log p(\hat{y}|g, Y_f^0), \quad (27)$$

where \mathcal{G} is the parameter space defined by the known noise-free input trajectory, namely

$$\mathcal{G} = \left\{ g \in \mathbb{R}^M \mid \begin{bmatrix} U_p \\ U_f \end{bmatrix} g = \begin{bmatrix} \mathbf{u}_{\text{ini}} \\ \mathbf{u} \end{bmatrix} \right\}. \quad (28)$$

Substituting (26) into (27), we have the equivalent optimization problem,

$$\begin{aligned}\underset{g \in \mathcal{G}, Y_f^0}{\text{minimize}} \quad & \log \det(\Sigma_y(g)) \\ & + \begin{bmatrix} Y_p g - \mathbf{y}_{\text{ini}} \\ Y_f g - Y_f^0 g \end{bmatrix}^\top \Sigma_y^{-1}(g) \begin{bmatrix} Y_p g - \mathbf{y}_{\text{ini}} \\ Y_f g - Y_f^0 g \end{bmatrix}.\end{aligned}\quad (29)$$

It is easy to see that the optimal value of Y_f^0 is Y_f regardless of the choice of g . So (29) is equivalent to

$$\underset{g \in \mathcal{G}}{\text{minimize}} \quad \log \det(\Sigma_y(g)) + \begin{bmatrix} Y_p g - \mathbf{y}_{\text{ini}} \\ \mathbf{0} \end{bmatrix}^\top \Sigma_y^{-1}(g) \begin{bmatrix} Y_p g - \mathbf{y}_{\text{ini}} \\ \mathbf{0} \end{bmatrix}. \quad (30)$$

In this objective function, the first term indicates how accurate the output estimates are. The second term represents how much the estimate deviates from the past output observations.

B. Iterative Computation of the Estimator

To find a computationally efficient algorithm to solve (30), we relax the problem and solve it with sequential quadratic programming (SQP) [33]. First, the covariance matrix Σ_y is approximated with its diagonal part, denoted by $\bar{\Sigma}_y$, i.e.,

$$(\bar{\Sigma}_y)_{i,j} = \begin{cases} (\Sigma_y)_{i,j}, & i = j \\ 0, & i \neq j \end{cases}. \quad (31)$$

Remark 2: This approximation holds exactly when the data matrices are constructed by truncating $(u_i^d, y_i^d)_{i=0}^{N-1}$ into sections of length L with no overlap, or using multiple independent trajectories of length L , instead of forming Hankel structures. This construction is known as the Page matrix [34] and it was shown in [17] that similar results to Theorem 1 still hold for Page matrices. The Hankel construction is able to use the data more efficiently, but leads to complex noise correlation, which is reflected in the non-diagonal structure of Σ_y . The comparison between the Hankel construction and the Page construction is, however, beyond the scope of this paper. See [34], [35] for more on this topic.

Remark 3: This approximation gives an upper bound on the log-det terms. According to Hadamard's inequality, since $\Sigma_y \in \mathbb{S}_{++}^L$,

$$\det(\Sigma_y) \leq \prod_{i=1}^L (\Sigma_y)_{i,i}. \quad (32)$$

So we have,

$$\log \det(\Sigma_y(g)) \leq \log \det(\bar{\Sigma}_y(g)). \quad (33)$$

In this way, problem (30) is approximated as

$$\begin{aligned}\underset{g \in \mathcal{G}}{\text{minimize}} \quad & L' \log \left(\|g\|_2^2 \right) + L_0 \log \left(\sigma^2 \|g\|_2^2 + \sigma_p^2 \right) \\ & + \frac{1}{\sigma^2 \|g\|_2^2 + \sigma_p^2} \|Y_p g - \mathbf{y}_{\text{ini}}\|_2^2.\end{aligned}\quad (34)$$

This problem can be readily solved by SQP. For each iteration, the following quadratic programming problem is solved.

$$\begin{aligned}g^{k+1} &= \underset{g}{\text{argmin}} \quad \lambda(g^k) \|g\|_2^2 + \|Y_p g - \mathbf{y}_{\text{ini}}\|_2^2 \\ \text{subject to} \quad & \begin{bmatrix} U_p \\ U_f \end{bmatrix} g = \begin{bmatrix} \mathbf{u}_{\text{ini}} \\ \mathbf{u} \end{bmatrix},\end{aligned}\quad (35)$$

where

$$\lambda(g^k) = \frac{L' \sigma_p^2}{\|g^k\|_2^2} + L \sigma^2. \quad (36)$$

The objective function in (34) is approximated by a quadratic function around g^k , making use of the local expansion $\log x \approx \log x_0 + \frac{1}{x_0}(x - x_0)$. The optimality conditions of (35) are:

$$\begin{bmatrix} F(g^k) & U^\top \\ U & \mathbf{0} \end{bmatrix} \begin{bmatrix} g^{k+1} \\ \nu^{k+1} \end{bmatrix} = \begin{bmatrix} Y_p^\top \mathbf{y}_{\text{ini}} \\ \tilde{\mathbf{u}} \end{bmatrix}, \quad (37)$$

where $\tilde{\mathbf{u}} = \text{col}(\mathbf{u}_{\text{ini}}, \mathbf{u})$, $F(g^k) = \lambda(g^k) \mathbb{I} + Y_p^\top Y_p$, and $\nu_{k+1} \in \mathbb{R}^L$ is the Lagrange multiplier. The closed-form solution is

thus given by

$$\begin{aligned} g^{k+1} &= (F^{-1} - F^{-1}U^T(UF^{-1}U^T)^{-1}UF^{-1})Y_p^T \mathbf{y}_{\text{ini}} \\ &\quad + F^{-1}U^T(UF^{-1}U^T)^{-1}\tilde{\mathbf{u}} \\ &=: \mathcal{P}(g^k)\mathbf{y}_{\text{ini}} + \mathcal{Q}(g^k)\tilde{\mathbf{u}}. \end{aligned} \quad (38)$$

This algorithm converges to a local minimum of problem (34).

C. Maximum Likelihood Data-Driven Simulation

Based on the derived maximum likelihood estimator of g , the step of solving the linear system (12) in Algorithm 1 can be replaced by solving the SQP problem (35). For simulation, the SQP problem can be initialized at the pseudoinverse solution g_{pinv} (15). This leads to the following algorithm for maximum likelihood data-driven simulation.

Algorithm 2 Maximum likelihood data-driven simulation: the signal matrix model

- 1: **Given:** $U_p, U_f, Y_p, Y_f, \sigma, \sigma_p, \epsilon$.
 - 2: **Input:** $\mathbf{u}_{\text{ini}}, \mathbf{y}_{\text{ini}}, \mathbf{u}$.
 - 3: $k \leftarrow 0, g^0 \leftarrow g_{\text{pinv}}$ from (15)
 - 4: **repeat**
 - 5: Calculate g^{k+1} with (38).
 - 6: $k \leftarrow k + 1$
 - 7: **until** $\|g^k - g^{k-1}\| < \epsilon \|g^{k-1}\|$
 - 8: **Output:** $g_{\text{SMM}} = g^k, \mathbf{y} = Y_f g^k$.
-

This algorithm gives the signal matrix model in the form of (11). The approximate maximum likelihood estimator (35) has the same $\|g\|_2^2$ penalization term as the least-norm problem (16). However, the estimate g_{SMM} does not lie in the solution space of the underdetermined system (12). The total least squares structure in (10b) leads to the penalization term $\|Y_p g - \mathbf{y}_{\text{ini}}\|_2^2$ in place of the hard constraint in (12).

D. Preconditioning of Data Matrices

In data-driven applications, it is usually assumed that abundant data are available, i.e., $N \gg L$. Under this scenario, the dimension of the parameter vector $g \in \mathbb{R}^M$, which needs to be optimized online, would be much larger than the length of the predicted output trajectory. This leads to high online computational complexity even to estimate a very short trajectory. On the other hand, only $2L$ independent basis vectors are needed to describe all the possible input-output trajectories of length L . It is possible to precondition the data matrices such that only $2L$ basis trajectories are used.

To do this, we propose the following strategy based on the SVD to compress the data such that the dimension of the parameter vector g is $2L$ regardless of the raw data length. Let

$$\begin{bmatrix} U \\ Y \end{bmatrix} = W S V^T \in \mathbb{R}^{2L \times M} \quad (39)$$

be the SVD of the data matrix. Define the compressed data matrices $\tilde{U}_p, \tilde{Y}_p \in \mathbb{R}^{L_0 \times 2L}$ and $\tilde{U}_f, \tilde{Y}_f \in \mathbb{R}^{L' \times 2L}$ such that

$$\text{col} \begin{pmatrix} \tilde{U}_p, \tilde{U}_f, \tilde{Y}_p, \tilde{Y}_f \end{pmatrix} = W S_{2L} \in \mathbb{R}^{2L \times 2L}, \quad (40)$$

where S_{2L} is the first $2L$ columns of S .

It is shown in the following proposition that Algorithm 2 with compressed data matrices obtains exactly the same output trajectory \mathbf{y} as with raw data matrices.

Proposition 1: Let the simulated trajectories with data matrices (U_p, Y_p, U_f, Y_f) and $(\tilde{U}_p, \tilde{Y}_p, \tilde{U}_f, \tilde{Y}_f)$ from Algorithm 2 be \mathbf{y} and $\tilde{\mathbf{y}}$ respectively. Then we have

$$\tilde{\mathbf{y}} = \mathbf{y}. \quad (41)$$

Proof: Define transformed data matrices $\bar{U}_p, \bar{Y}_p, \bar{U}_f, \bar{Y}_f$ and \bar{Y}_f such that

$$\text{col}(\bar{U}_p, \bar{Y}_p, \bar{U}_f, \bar{Y}_f) = W S. \quad (42)$$

Then the relations between the data matrices are given by

$$\begin{aligned} \text{col}(U_p, Y_p, U_f, Y_f) &= \text{col}(\tilde{U}_p, \tilde{U}_f, \tilde{Y}_p, \tilde{Y}_f) V_{2L}^T, \\ \text{col}(U_p, Y_p, U_f, Y_f) &= \text{col}(\bar{U}_p, \bar{Y}_p, \bar{U}_f, \bar{Y}_f) V^T, \\ \text{col}(\bar{U}_p, \bar{Y}_p, \bar{U}_f, \bar{Y}_f) &= \left[\text{col}(\tilde{U}_p, \tilde{U}_f, \tilde{Y}_p, \tilde{Y}_f) \quad \mathbf{0} \right]. \end{aligned} \quad (43)$$

where V_{2L} denotes the first $2L$ columns of V .

Denote the variables with the compressed data matrices by a tilde, and the variables with the transformed data matrices by a bar. Since $V_{2L}^T V_{2L} = \mathbb{I}$, we have

$$g_{\text{pinv}} = V_{2L} \tilde{g}_{\text{pinv}}. \quad (44)$$

This leads to $\|g_{\text{pinv}}\|_2^2 = \|\tilde{g}_{\text{pinv}}\|_2^2$, and thus $\lambda(g^0) = \lambda(\tilde{g}^0)$.

Suppose at the k -th iteration, $\lambda(g^k) = \lambda(\tilde{g}^k)$. Due to the orthogonality of V and the sparsity structure of \bar{U} and \bar{Y}_p , we have

$$g^{k+1} = V \bar{g}^{k+1}, \quad \bar{g}^{k+1} = [\tilde{g}^{k+1} \quad \mathbf{0}]. \quad (45)$$

This leads to

$$g^{k+1} = V_{2L} \tilde{g}^{k+1}, \quad \|g^{k+1}\|_2^2 = \|\tilde{g}^{k+1}\|_2^2. \quad (46)$$

Thus for all k , we have $g^k = V_{2L} \tilde{g}^k$. Therefore, the simulated trajectory satisfies

$$\mathbf{y} = Y_f g^k = \tilde{Y}_f \tilde{g}^k = \tilde{\mathbf{y}}. \quad (47)$$

■
Remark 4: It can be seen from the proof that $\bar{\Sigma}_y(g) = \bar{\Sigma}_y(\tilde{g})$. So with compressed data matrices, the output trajectory estimate has the same covariance as the raw data matrices when Page matrices are used, and the same diagonal components when Hankel matrices are used.

The signal matrix model (Algorithm 2), together with the above data compression scheme, can be applied to various problems in system identification and control. In the following two sections, two approaches are discussed to apply this model to problems in kernel-based identification and receding horizon predictive control.

V. KERNEL-BASED IDENTIFICATION WITH THE SIGNAL MATRIX MODEL

We propose here a kernel-based system identification method that identifies an FIR model of the system [36]. By combining the kernel-based regularization with the signal matrix model, model fitting is improved compared to the conventional kernel method based on least squares, when the truncation error is large or the past inputs are unknown.

A. Impulse Response Estimation

Consider the problem of estimating the impulse response model $(h_i)_{i=0}^{\infty}$ of a system from data. The output y_t is given by

$$y_t = \sum_{i=0}^{\infty} h_i u_{t-i}. \quad (48)$$

The conventional approach is to formulate a linear regression to estimate a finite truncation of the impulse response

$$\underbrace{\begin{bmatrix} y_0^d \\ y_1^d \\ \vdots \\ y_{N-1}^d \end{bmatrix}}_{y_N} = \underbrace{\begin{bmatrix} u_0^d & u_{-1}^d & \cdots & u_{1-n}^d \\ u_1^d & u_0^d & \cdots & u_{2-n}^d \\ \vdots & \vdots & \ddots & \vdots \\ u_{N-1}^d & u_{N-2}^d & \cdots & u_{N-n}^d \end{bmatrix}}_{\Phi_N} \underbrace{\begin{bmatrix} h_0 \\ h_1 \\ \vdots \\ h_{n-1} \end{bmatrix}}_h, \quad (49)$$

where n is the length of the impulse response to be estimated. The regression problem can then be solved by least squares. There are two main assumptions underlying this formulation: 1) the truncation error of the finite impulse response is negligible, i.e., $h_i \approx 0$ for all $i \geq n$; and 2) the past input trajectory $(u_i^d)_{i=1-n}^{-1}$ is known. With these two assumptions, the least-squares solution is known to be the best unbiased estimator when i.i.d. Gaussian output noise is present [2].

However, these assumptions may not be satisfied in practice. When the internal dynamics matrix A has a large condition number, a very long impulse response sequence is needed to remove the truncation error even for a low-order system. In this case, the least-squares algorithm may become impractical due to limited data length and/or computation power. If the truncation error is not negligible, the estimator is not correct, i.e., in the noise-free case, the estimate does not coincide with the true system. When the past inputs are unknown, the first $(n-1)$ output measurements cannot be used. In non-parametric estimation, the size n is usually comparable to N , in which case the data efficiency is substantially affected. Similar assumptions are required for non-parametric methods in the frequency domain as well, where periodic input signals are assumed and a sufficiently long dataset is needed to avoid aliasing.

In this work, we propose using the signal matrix model to estimate the impulse response with

$$\mathbf{u}_{\text{ini}} = \mathbf{0}, \mathbf{y}_{\text{ini}} = \mathbf{0}, \mathbf{u} = \text{col}(1, \mathbf{0}), \sigma_p = 0, L' = n. \quad (50)$$

Then the output trajectory \mathbf{y} is an estimate of the impulse response h of length n of the system [28]. It is noted that this approach requires neither of the assumptions for the least-squares method. Instead of requiring a long past input

sequence, this approach uses a small part of the data to estimate the initial condition of each trajectory section. In fact, the estimator is correct and unbiased for an arbitrary length n and unknown past inputs as shown in Theorem 1(e), as long as the persistency of excitation condition is satisfied.

B. Kernel-Based Regularization

The FIR model is widely used in kernel-based identification methods, where the estimates learned from data are combined with a prior of the impulse response that encodes typical system characteristics including low-complexity and exponential stability. Consider an estimate from data with the following statistics

$$h \sim \mathcal{N}(\hat{h}, \Sigma_d), \quad (51)$$

and assume a prior distribution on h defined by the kernel Σ_k as

$$h \sim \mathcal{N}(\mathbf{0}, \Sigma_k). \quad (52)$$

The kernel Σ_k is usually parametrized by a small number of design parameters η [37].

Then the optimal linear combination of the kernel-based prior and the data-based estimator in the minimum mean square error sense is given by

$$h \sim \mathcal{N}(K\hat{h}, \Sigma_{\text{opt}}), \quad (53)$$

where $K = \Sigma_k (\Sigma_k + \Sigma_d)^{-1}$ is the Kalman gain and $\Sigma_{\text{opt}} = \Sigma_k - \Sigma_k (\Sigma_k + \Sigma_d)^{-1} \Sigma_k$. The least-squares solution is typically used as the data-based estimate with

$$\hat{h} = (\Phi_N^T \Phi_N)^{-1} \Phi_N^T y_N, \Sigma_d = \sigma^2 (\Phi_N^T \Phi_N)^{-1}. \quad (54)$$

The posterior mean of (53) then gives the well-known closed-form solution of the kernel-based regularization [38]

$$h_{\text{LS-ker}} = K\hat{h} = (\Phi_N^T \Phi_N + \sigma^2 \Sigma_k^{-1})^{-1} \Phi_N^T y_N, \quad (55)$$

which is also the solution to the following regularized least-squares problem

$$h_{\text{LS-ker}} = \underset{h}{\text{argmin}} \sigma^{-2} \|y_N - \Phi_N h\|_2^2 + h^T \Sigma_k^{-1} h. \quad (56)$$

In fact, any stochastic estimator of the impulse response can be combined with the kernel prior. In this work, to overcome the limitations of the least-squares regression discussed in the previous subsection, we apply the impulse response trajectory \mathbf{y} simulated with the signal matrix model as the data-based estimate. Then according to (22), we have

$$\hat{h} = \mathbf{y}, \Sigma_d = \Sigma_{y_f}, \quad (57)$$

where $\Sigma_{y_f} \in \mathbb{S}_{++}^{L'}$ denotes the last L' rows and columns of Σ_y .

Then the kernel-based estimate of the FIR model with the signal matrix model is given by

$$\begin{aligned} h_{\text{SMM-ker}} &= \underset{h}{\text{argmin}} (h - \mathbf{y})^T \Sigma_{y_f}^{-1} (h - \mathbf{y}) + h^T \Sigma_k^{-1} h \\ &= \Sigma_k (\Sigma_k + \Sigma_{y_f})^{-1} \mathbf{y}. \end{aligned} \quad (58)$$

To determine the hyperparameters in the kernel design $\Sigma_k = \Sigma_k(\eta)$, the empirical Bayes method is applied [36]. This

method maximizes the marginal probability of observing \hat{h} given the kernel design parameters η :

$$\hat{h}|\eta \sim \mathcal{N}(\mathbf{0}, \Sigma_k(\eta) + \Sigma_{y_f}). \quad (59)$$

This leads to

$$\begin{aligned} \eta^* &= \underset{\eta}{\operatorname{argmin}} -\log p(\hat{h}|\eta) \\ &= \underset{\eta}{\operatorname{argmin}} \log \det(\Sigma_k(\eta) + \Sigma_{y_f}) + \mathbf{y}^\top (\Sigma_k(\eta) + \Sigma_{y_f})^{-1} \mathbf{y}. \end{aligned} \quad (60)$$

When the dimension of η is small, this optimization problem can be solved by grid search, otherwise nonlinear optimization can be employed.

Building upon the previous steps, the following algorithm is proposed to identify the FIR model with the data-driven kernel-based method. Note that when $\sigma_p = 0$, the adaptive weighting $\lambda(g^k)$ is fixed. Therefore, only one iteration is needed in Algorithm 2.

Algorithm 3 Kernel-based impulse response estimation with the signal matrix model

- 1: **Given:** $U_p, U_f, Y_p, Y_f, \sigma, \epsilon$.
- 2: $\mathbf{u}_{\text{ini}} \leftarrow \mathbf{0}, \mathbf{y}_{\text{ini}} \leftarrow \mathbf{0}, \mathbf{u} \leftarrow \operatorname{col}(1, \mathbf{0}), \sigma_p \leftarrow 0$
- 3: Compute \mathbf{y} and g_{SMM} by Algorithm 2.
- 4: Calculate $\Sigma_{y_f}(g_{\text{SMM}})$ by (24).
- 5: Solve (60) for η^* .
- 6: **Output:** $h_{\text{SMM-ker}} = \Sigma_k(\eta^*) (\Sigma_k(\eta^*) + \Sigma_{y_f}(g_{\text{SMM}}))^{-1} \mathbf{y}$.

C. Numerical Results

In this subsection, the proposed algorithm is tested against least-squares-based estimates by applying it to numerical examples. The tuned/correlated (TC) kernel structure

$$(\Sigma_k)_{i,j} = \alpha \min(\beta^i, \beta^j), \quad \eta = \operatorname{col}(\alpha, \beta) \quad (61)$$

is used [38]. We compare the following four algorithms: 1) *LS*: least-squares estimate (54), 2) *LS-TC*: kernel-based/least-squares estimate (55) with the TC kernel, 3) *SMM*: signal matrix model estimate (Algorithm 2 with (50)), and 4) *SMM-TC*: kernel-based/signal matrix model estimate (Algorithm 3) with the TC kernel. The parameters used in the simulation are $N = 50, L_0 = 4, n = L' = 11, \sigma^2 = 0.01$. The identification data are generated with unit i.i.d Gaussian input signals. For each case, 100 Monte Carlo simulations are conducted.

In the first example, we consider the following fourth-order LTI system tested in [36]

$$G_1(z) = \frac{0.1159(z^3 + 0.5z)}{z^4 - 2.2z^3 + 2.42z^2 - 1.87z + 0.7225}. \quad (62)$$

This system is relatively slow. The truncation error is significant when $n = 11$ is selected. First, the data-based estimates *LS* and *SMM* are compared under the noise-free case, and the results are shown in Figure 1(a). It can be clearly seen that the least-squares estimator is not correct due to the presence of truncation errors, whereas the *SMM* estimator is correct. When the noise is present, all four algorithms are compared

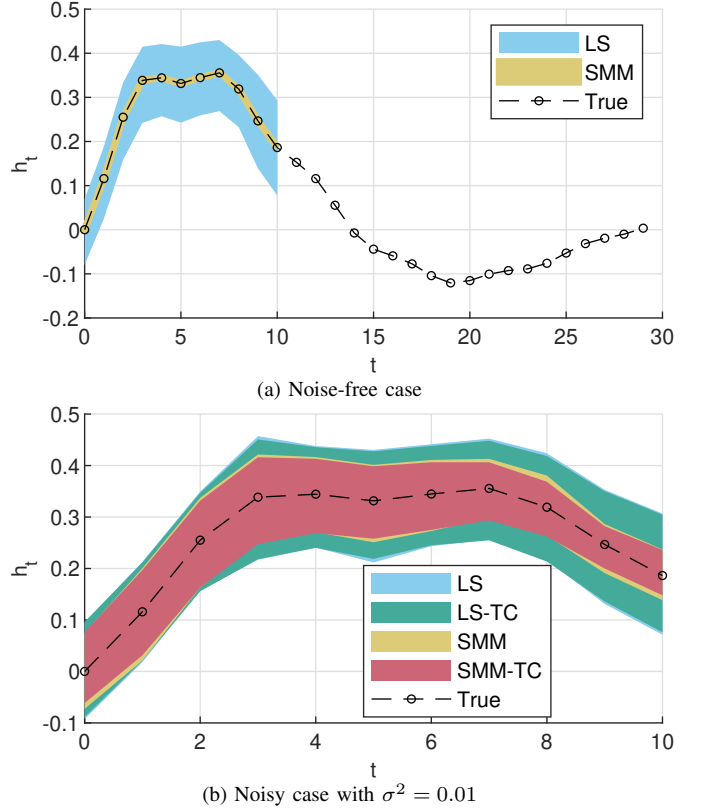


Fig. 1. Comparison of impulse response estimation with truncation errors. Colored area: estimates within two standard deviation.

in Figure 1(b). The estimators with the signal matrix model have smaller variance compared to the least-squares ones.

In the second example, we focus on the effect of unknown past inputs by investigating a faster LTI system used in [36]

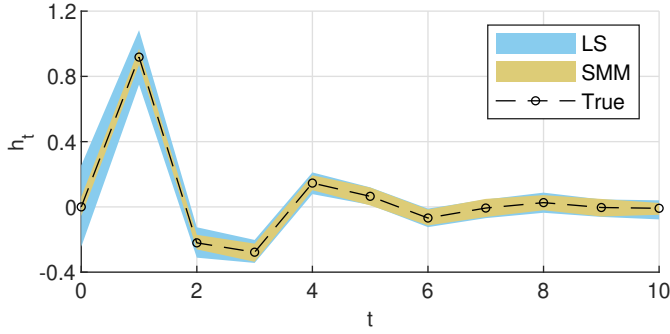
$$G_2(z) = \frac{0.9183z}{z^2 + 0.24z + 0.36}. \quad (63)$$

In this case, the truncation error is already negligible at $n = 11$, but we assume the past inputs are unknown. The results of the estimation are illustrated in Figure 2. As can be observed from Figure 2(a), the result of the *SMM* algorithm is more accurate than the *LS* algorithm, especially for the first four coefficients. Regularizing with the TC kernel prior improves the estimation quality for the tail of the impulse response as shown in Figure 2(b).

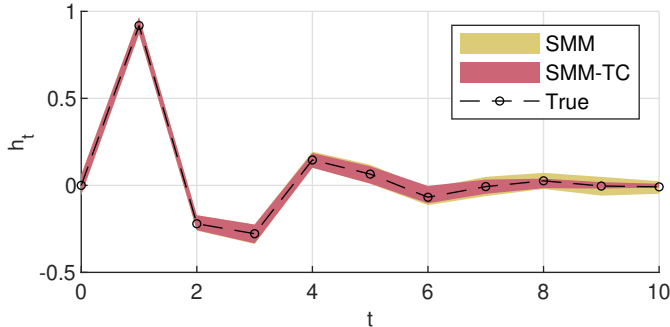
To quantitatively assess the performance of different algorithms, we quantify the model fitting by

$$W = 100 \cdot \left(1 - \left[\frac{\sum_{i=1}^n (h_i - \hat{h}_i)^2}{\sum_{i=1}^n (h_i - \bar{h})^2} \right]^{1/2} \right), \quad (64)$$

where h_i are the true impulse response coefficients, \hat{h}_i are the estimated coefficients, and \bar{h} is the mean of the true coefficients. The boxplots of model fitting for both examples are plotted in Figure 3. For comparison, the case with known past inputs is also plotted for example 2. The *SMM* and *SMM-TC* algorithms perform better than the *LS* and *LS-TC* algorithms when the truncation error is large or the past inputs are unknown. However, when both assumptions of the least



(a) Comparison between SMM and least-squares estimates



(b) Effect of kernel regularization on the SMM method

Fig. 2. Comparison of impulse response estimation with unknown past inputs. Colored area: estimates within two standard deviation.

squares are satisfied, the least-squares-based methods perform slightly better than the methods with the signal matrix model. This is due to the fact that part of the data is used to estimate the initial condition in Algorithm 2, whereas it is known for the least-squares method.

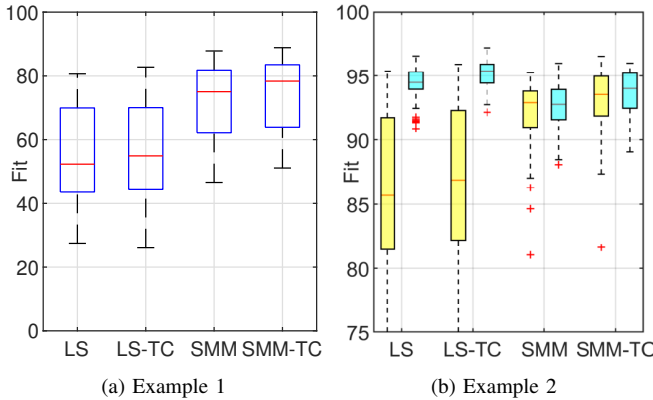


Fig. 3. Comparison of model fitting for both examples with 100 simulations. In (b), yellow: unknown past input, cyan: known past inputs.

VI. DATA-DRIVEN PREDICTIVE CONTROL WITH THE SIGNAL MATRIX MODEL

In this section, the signal matrix model is used as the predictor in receding horizon predictive control. As discussed in Section IV, the predictor in the unregularized DeePC problem (14) becomes ill-conditioned when noise is present. In the following subsections, we will present two existing methods to remedy this problem, and compare the control performance with the optimal predictor proposed in this paper.

A. Pseudoinverse and Regularized Algorithms

There are mainly two types of existing algorithms to extend (14) to the noisy case: the data-driven subspace predictive control and the regularized DeePC algorithm.

The subspace predictive control approach [27] uses the pseudoinverse solution of g in the predictor instead of the underdetermined linear equality constraints as follows

$$\begin{aligned} & \underset{\mathbf{u}, \mathbf{y}}{\text{minimize}} && J_{\text{ctr}}(\mathbf{u}, \mathbf{y}) \\ & \text{subject to} && \mathbf{y} = Y_f g_{\text{pinv}}(\mathbf{u}; \mathbf{u}_{\text{ini}}, \mathbf{y}_{\text{ini}}), \mathbf{u} \in \mathcal{U}, \mathbf{y} \in \mathcal{Y}, \end{aligned} \quad (65)$$

where $g_{\text{pinv}}(\cdot)$ is defined in (15). Multiple applications have been studied with similar algorithms (e.g., [39], [40]). However, as discussed in Section IV, $g_{\text{pinv}}(\cdot)$ is not guaranteed to be an effective choice of g for systems with noise.

The regularized DeePC algorithm [19] adds additional regularization terms in the objective in order to regularize both the norm of g and the slack variable needed to satisfy (10b):

$$\begin{aligned} & \underset{\mathbf{u}, \mathbf{y}, g, \hat{\mathbf{y}}_{\text{ini}}}{\text{minimize}} && J_{\text{ctr}}(\mathbf{u}, \mathbf{y}) + \lambda_g \|g\|_p^p + \lambda_y \|\hat{\mathbf{y}}_{\text{ini}} - \mathbf{y}_{\text{ini}}\|_p^p \\ & \text{subject to} && \begin{bmatrix} U_p \\ Y_p \\ U_f \\ Y_f \end{bmatrix} g = \begin{bmatrix} \mathbf{u}_{\text{ini}} \\ \hat{\mathbf{y}}_{\text{ini}} \\ \mathbf{u} \\ \mathbf{y} \end{bmatrix}, \mathbf{u} \in \mathcal{U}, \mathbf{y} \in \mathcal{Y}, \end{aligned} \quad (66)$$

where p is usually selected as 1 or 2. This algorithm can be interpreted as an MPC algorithm acting on the implicit parametric model structure (9) and (10), where the objective is a trade-off between the control performance objective J_{ctrl} and the parameter estimation objective

$$J_{\text{id, DeePC}} := \lambda \|g\|_p^p + \|\hat{\mathbf{y}}_{\text{ini}} - \mathbf{y}_{\text{ini}}\|_p^p, \lambda = \frac{\lambda_g}{\lambda_y}. \quad (67)$$

The set of underdetermined model parameters ($g, \hat{\mathbf{y}}_{\text{ini}}$) are then estimated adaptively in the MPC algorithm. This algorithm is also shown to be effective in multiple applications (e.g., [20], [21]). However, there are two main problems associated with it. First, the model parameters are optimized in an optimistic manner in that as regularization terms, the estimator is biased towards those that predict better control performance. However, the system behaviors should be independent of the control task. Second, tuning of the regularization parameters is a very hard problem. To the best of our knowledge, there is no practical approach proposed to tune λ_g and λ_y beforehand, and unfortunately the control performance is known to be very sensitive to the regularization parameters [20].

Remark 5: The same data compression scheme as discussed in IV-D is applicable to these two algorithms as well.

B. An Optimal Tuning-Free Approach

To address the concerns regarding the two existing methods discussed in the previous subsection, we propose a receding horizon predictive control scheme with the signal matrix model as the predictor. This directly leads to

$$\begin{aligned} & \underset{\mathbf{u}, \mathbf{y}}{\text{minimize}} && J_{\text{ctr}}(\mathbf{u}, \mathbf{y}) \\ & \text{subject to} && \mathbf{y} = Y_f g_{\text{SMM}}(\mathbf{u}; \mathbf{u}_{\text{ini}}, \mathbf{y}_{\text{ini}}), \mathbf{u} \in \mathcal{U}, \mathbf{y} \in \mathcal{Y}, \end{aligned} \quad (68)$$

where $g_{\text{SMM}}(\cdot)$ is obtained by Algorithm 2. However, unlike the pseudoinverse predictor where $g_{\text{pinv}}(\cdot)$ is linear with respect to \mathbf{u} , the maximum likelihood predictor $g_{\text{SMM}}(\cdot)$ involves an iterative algorithm which cannot be expressed as an equality constraint explicitly.

To solve this problem, we notice that the l_2 -norm of g does not change much throughout the receding horizon control, and the algorithm is only iterative with respect to $\|g\|_2^2$. So in a receding horizon context, it makes sense to warm-start the optimization problem from the g -value at the previous time instant. Then, $g_{\text{SMM}}(\cdot)$ can be closely approximated by the solution of (38) after the first iteration, i.e.,

$$g^t(\mathbf{u}; \mathbf{u}_{\text{ini}}, \mathbf{y}_{\text{ini}}, g^{t-1}) = \mathcal{P}(g^{t-1}) \mathbf{y}_{\text{ini}} + \mathcal{Q}(g^{t-1}) \tilde{\mathbf{u}}, \quad (69)$$

where, with an abuse of notation, $g^t(\cdot)$ denotes the approximation of $g_{\text{SMM}}(\cdot)$ with one iteration at time instant t . In this way, the SMM predictor is approximated by a linear equality constraint that can be efficiently solved within a quadratic program. Thus, the proposed approach solves the following optimization problem at each time step

$$\begin{aligned} & \underset{\mathbf{u}, \mathbf{y}}{\text{minimize}} && J_{\text{ctr}}(\mathbf{u}, \mathbf{y}) \\ & && \mathbf{y} = Y_f g^t, \\ & \text{subject to} && g^t = \mathcal{P}(g^{t-1}) \mathbf{y}_{\text{ini}} + \mathcal{Q}(g^{t-1}) \tilde{\mathbf{u}}, \\ & && \mathbf{u} \in \mathcal{U}, \mathbf{y} \in \mathcal{Y}. \end{aligned} \quad (70)$$

The parameter estimation part (67) in regularized DeePC has the same form as the maximum likelihood estimator (35) with $p = 2$, which leads to the predictor in (70). However, our proposed method avoids the aforementioned shortcomings with the regularized DeePC algorithm: 1) the parameter estimation part is isolated from the control performance objective and placed in the predictor itself; 2) the problem of hyperparameter tuning is avoided by deriving the coefficients statistically, which requires only information about the noise levels of the offline data σ^2 and the online measurements σ_p^2 .

C. Numerical Results

In this subsection, we compare the control performance of three receding horizon predictive control algorithms: 1) *Sub-PC*: subspace predictive control (65), 2) *DeePC*: regularized DeePC (66), and 3) *SMM-PC*: predictive control with the signal matrix model (70). In *DeePC*, the algorithm is tested on a nine-point logarithmic grid of λ_g between 10 and 1000. In this example, the control performance is found to not be sensitive to the value of λ_y , so a fixed value of $\lambda_y = 1000$ is used. In *SMM-PC*, it is assumed that the noise levels σ^2 and σ_p^2 are known. To benchmark the performance, we also consider the ideal MPC algorithm (denoted by *MPC*), where both the true state-state model and the noise-free state measurements are available. The result of this benchmark algorithm is thus deterministic and gives the best possible control performance with receding horizon predictive control.

In this example, we consider the LTI system (62). Unless otherwise specified, the following parameters are used in the simulation

$$N = 200, L_0 = 4, L' = 11, \sigma^2 = \sigma_p^2 = 1, Q = R = 1.$$

No input and output constraints are enforced, i.e., $\mathcal{U} = \mathbb{R}^{L'u}$ and $\mathcal{Y} = \mathbb{R}^{L'y}$. A sinusoidal reference trajectory $r_t = 0.5 \sin(\frac{\pi}{10}t)$ is to be tracked. The offline data are generated with unit i.i.d Gaussian input signals. For each case, 100 Monte Carlo simulations are conducted. In each run, 60 time steps are simulated. The control performance is assessed by the true stage cost over all time steps, i.e.,

$$J = \sum_{k=0}^{N_c-1} \left(\|y_k^0 - r_k\|_Q^2 + \|u_k\|_R^2 \right), \quad (71)$$

where $N_c = 60$ and y_k^0 is the noise-free measurement at time k . When comparing the closed-loop performance, the best choices of λ_g in *DeePC* are selected with an oracle for each run as plotted in Figure 4 for different noise levels. It can be seen that, even for the same control task, the optimal value of this hyperparameter is not only sensitive to the noise level but also to the specific realization of the noise. This makes the tuning process difficult in practice.

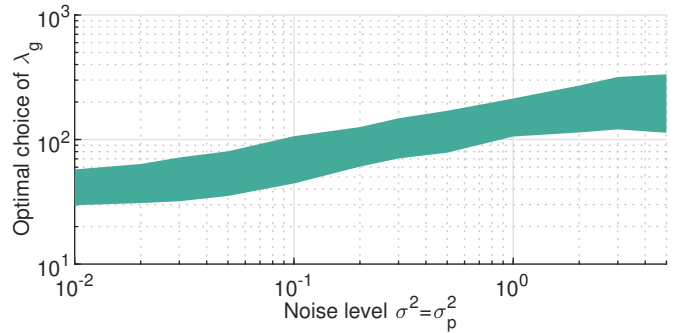


Fig. 4. The best choice of λ_g in *DeePC* for different noise levels. Colored area: values within one standard deviation.

The optimization problems are all formulated as quadratic programming problems and solved by MOSEK. The computation time for all three algorithms is similar. The effect of the proposed data compression scheme in Section IV-D is illustrated in Figure 5 with the example of *SMM-PC*. By applying the preconditioning, the computational complexity no longer depends on the data size N .

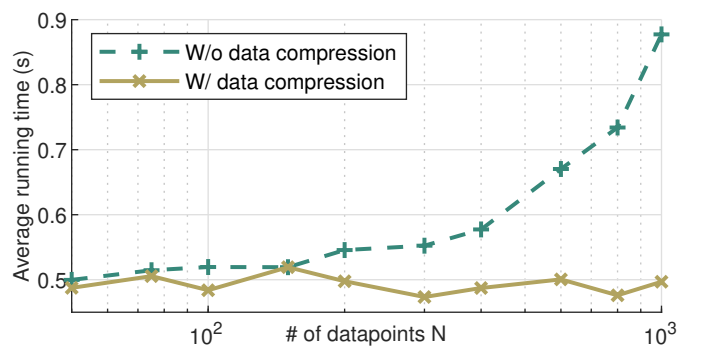


Fig. 5. Average computation time of *SMM-PC* with and without the data compression scheme.

The closed-loop input-output trajectories of different control algorithms are plotted in Figure 6. The closed-loop trajectories are characterized by the range within one standard deviation of

the Monte-Carlo simulation. The *SMM-PC* algorithm obtains the closest match with the benchmark trajectory *MPC*. *Sub-PC* applies more aggressive control inputs which results in much larger input costs, whereas the control strategy in *DeePC* is more conservative which results in significantly larger tracking errors. The *SMM-PC* trajectories also have the smallest variance. The boxplot of the control performance measure J is shown in Figure 7, which confirms that *SMM-PC* performs better than *Sub-PC* and *DeePC* in this control task.

The effects of different offline data sizes N and noise levels σ^2, σ_p^2 are investigated in Figure 8. As shown in Figure 8(a), the control performance of *SMM-PC* is not sensitive to the number of datapoints and performs uniformly better among the three algorithms. In fact, good performance is already obtained at only $N = 50$. *DeePC* does not perform very well with small data sizes but gets a similar performance to *SMM-PC* when $N \geq 600$. *Sub-PC* cannot achieve a satisfying result even with a large data size because a larger N can only average out the effect of offline noise σ^2 but not online measurement noise σ_p^2 , which is problematic to deal with in *Sub-PC*. Figure 8(b) shows that all three algorithms perform similarly at low noise levels as they are all stochastic variants of the noise-free algorithm (14). *SMM-PC* obtains slightly worse results under low noise levels ($\sigma^2 = \sigma_p^2 < 0.3$) compared to the optimally tuned *DeePC* with an oracle, but the performance improvement is significant for higher noise levels.

VII. CONCLUSIONS

In this work, we propose a novel statistical framework to estimate data-driven models from large noise-corrupted datasets. This is formulated as a maximum likelihood estimation problem. The problem is solved efficiently by approximating it as a sequential quadratic program with data compression. This framework extends the current works on data-driven methods to noisy data by providing an optimal solution to the underdetermined implicit model structure and establishing the signal matrix model.

With the signal matrix model, two approaches in kernel-based system identification and receding horizon control are developed. They obtain an impulse response estimate with less restrictive assumptions and an effective tuning-free data-driven receding horizon control algorithm respectively. The results from these two approaches demonstrate that the proposed framework can improve the state-of-the-art methods in both data-driven simulation and control in the presence of noisy data.

APPENDIX I DERIVATION OF Σ_y

Let $\zeta_i \in \mathbb{R}^L$, $i = 1, \dots, LM$ be the i -th column of $(g^\top \otimes \mathbb{I})$, $\mathcal{S} = \left\{ (i, j) \mid (\text{vec}(Y))_i = (\text{vec}(Y))_j \right\}$, and $\Sigma_{y1} = (g^\top \otimes \mathbb{I}) \Sigma_{yd} (g \otimes \mathbb{I})$. According to (23), we have

$$\Sigma_{y1} = \sigma^2 \sum_{(i,j) \in \mathcal{S}} \zeta_i \zeta_j^\top. \quad (72)$$

Let the i -th and the j -th entries of $\text{vec}(Y)$ correspond to the (q, r) -th and the (s, t) -th entries of Y respectively, i.e., $i = (r-1)L + q$, $j = (t-1)L + s$. From the Hankel structure, the pair $(i, j) \in \mathcal{S}$ iff $q + r = s + t$. According to the structure of $(g^\top \otimes \mathbb{I})$, we have $\zeta_i = g_r \mathbf{e}_q$, $\zeta_j = g_t \mathbf{e}_s$, where $\mathbf{e}_q \in \mathbb{R}^L$ is the unit vector with q -th non-zero entry, and similarly for \mathbf{e}_s . Thus,

$$\Sigma_{y1} = \sigma^2 \sum_{q+r=s+t} g_r g_t \mathbf{e}_q \mathbf{e}_s^\top. \quad (73)$$

So the (q, s) -th entry of Σ_{y1} is given by

$$(\Sigma_{y1})_{q,s} = \sigma^2 \sum_{q+r=s+t} g_r g_t, \quad (74)$$

which directly leads to (24).

REFERENCES

- [1] Z.-S. Hou and Z. Wang, "From model-based control to data-driven control: Survey, classification and perspective," *Information Sciences*, vol. 235, pp. 3–35, 2013.
- [2] L. Ljung, *System identification: theory for the user*. Prentice Hall, 1999.
- [3] G. C. Chow *et al.*, *Analysis and control of dynamic economic systems*. Wiley, 1975.
- [4] G. C. Goodwin and K. S. Sin, *Adaptive filtering prediction and control*. Courier Corporation, 2014.
- [5] H. Hjalmarsson, "From experiment design to closed-loop control," *Automatica*, vol. 41, no. 3, pp. 393–438, 2005.
- [6] R. Sutton. (2019, Mar.) The bitter lesson. Blog. [Online]. Available: <http://www.incompleteideas.net/Incldeas/BitterLesson.html>
- [7] M. G. Safonov and Tung-Ching Tsao, "The unfalsified control concept and learning," *IEEE Transactions on Automatic Control*, vol. 42, no. 6, pp. 843–847, 1997.
- [8] H. Hjalmarsson, M. Gevers, S. Gunnarsson, and O. Lequin, "Iterative feedback tuning: theory and applications," *IEEE Control Systems Magazine*, vol. 18, no. 4, pp. 26–41, 1998.
- [9] M. Campi, A. Lecchini, and S. Savaresi, "Virtual reference feedback tuning: a direct method for the design of feedback controllers," *Automatica*, vol. 38, no. 8, pp. 1337–1346, 2002.
- [10] B. Recht, "A tour of reinforcement learning: The view from continuous control," *Annual Review of Control, Robotics, and Autonomous Systems*, vol. 2, no. 1, pp. 253–279, 2019.
- [11] M. G. Lagoudakis and R. Parr, "Least-squares policy iteration," *Journal of machine learning research*, vol. 4, no. Dec, pp. 1107–1149, 2003.
- [12] W. B. Powell, *Approximate Dynamic Programming: Solving the curses of dimensionality*. Wiley, 2007, vol. 703.
- [13] H. J. V. Waarde, J. Eising, H. L. Trentelman, and M. K. Camlibel, "Data informativity: a new perspective on data-driven analysis and control," *IEEE Transactions on Automatic Control*, 2020.
- [14] J. C. Willems, P. Rapisarda, I. Markovsky, and B. L. M. De Moor, "A note on persistency of excitation," *Systems & Control Letters*, vol. 54, no. 4, pp. 325–329, 2005.
- [15] I. Markovsky and P. Rapisarda, "Data-driven simulation and control," *International Journal of Control*, vol. 81, no. 12, pp. 1946–1959, 2008.
- [16] C. De Persis and P. Tesi, "Formulas for data-driven control: Stabilization, optimality, and robustness," *IEEE Transactions on Automatic Control*, vol. 65, no. 3, pp. 909–924, 2020.
- [17] H. J. van Waarde, C. De Persis, M. K. Camlibel, and P. Tesi, "Willems' fundamental lemma for state-space systems and its extension to multiple datasets," *IEEE Control Systems Letters*, vol. 4, no. 3, pp. 602–607, 2020.
- [18] E. F. Camacho and C. Bordons, *Model predictive control: classical, robust and stochastic*. Springer, 2016.
- [19] J. Coulson, J. Lygeros, and F. Dörfler, "Data-enabled predictive control: In the shallows of the DeePC," in *2019 18th European Control Conference (ECC)*, 2019, pp. 307–312.
- [20] L. Huang, J. Coulson, J. Lygeros, and F. Dörfler, "Data-enabled predictive control for grid-connected power converters," in *2019 IEEE 58th Conference on Decision and Control (CDC)*, 2019, pp. 8130–8135.
- [21] J. Coulson, J. Lygeros, and F. Dörfler, "Regularized and distributionally robust data-enabled predictive control," in *2019 IEEE 58th Conference on Decision and Control (CDC)*, 2019, pp. 2696–2701.

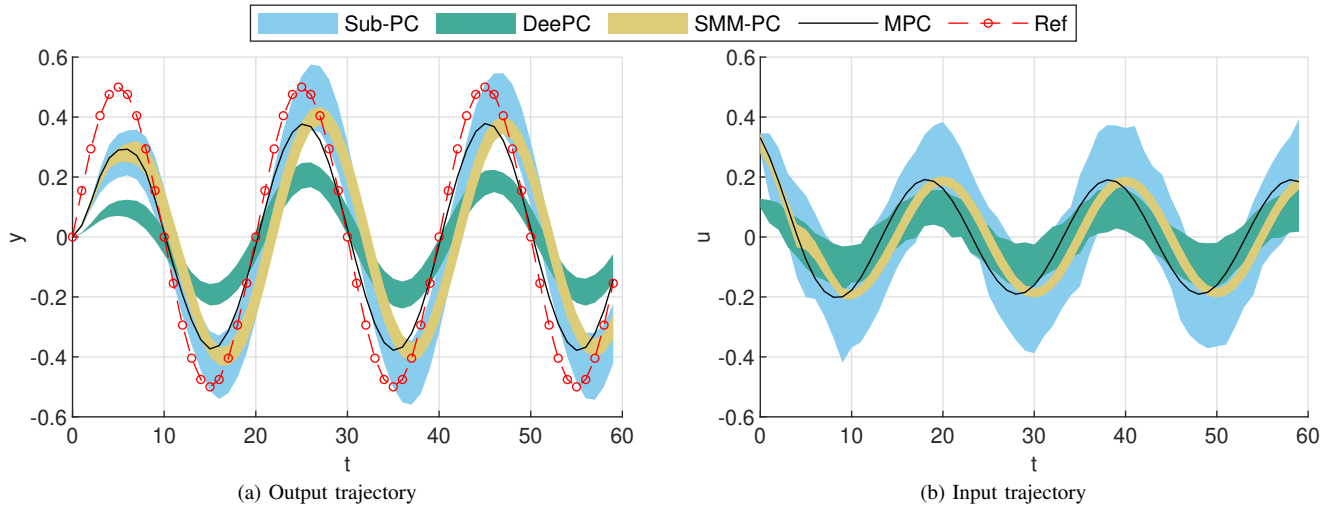


Fig. 6. Comparison of closed-loop input-output trajectories with different control algorithms. Colored area: trajectories within one standard deviation.

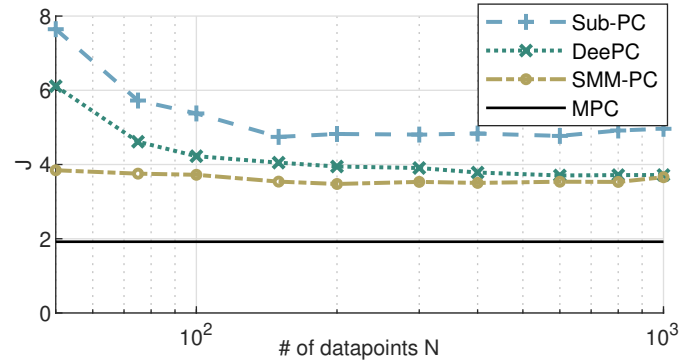
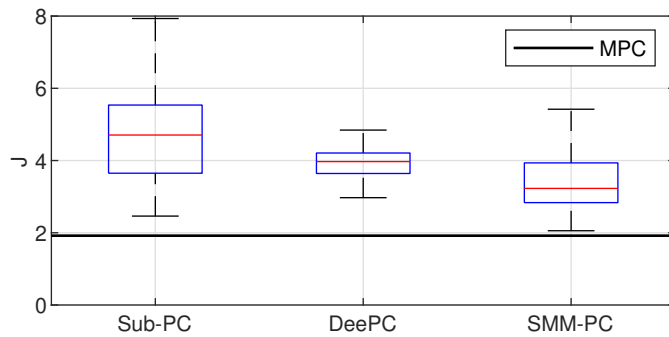


Fig. 7. Comparison of the control performance in terms of total stage costs J with different control algorithms with 100 simulations ($\sigma^2 = \sigma_p^2 = 1$, $N = 200$).

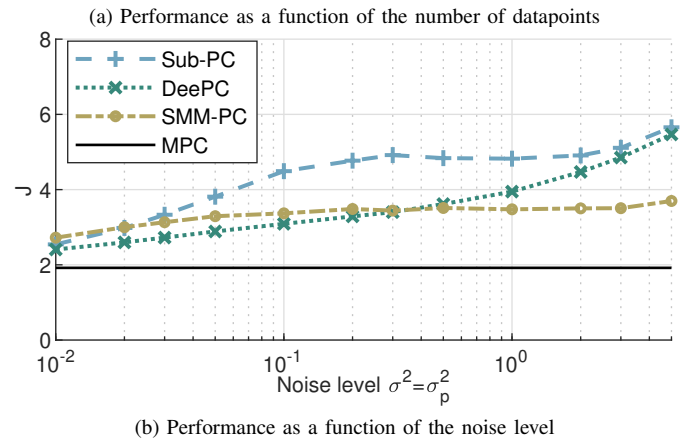


Fig. 8. The effect of different offline data sizes and noise levels on the control performance.

[22] D. Alpage, F. Dörfler, and J. Lygeros, “An extended Kalman filter for data-enabled predictive control,” *IEEE Control Systems Letters*, vol. 4, no. 4, pp. 994–999, 2020.

[23] J. Berberich, J. Koehler, M. A. Muller, and F. Allgower, “Data-driven model predictive control with stability and robustness guarantees,” *IEEE Transactions on Automatic Control*, 2020.

[24] M. Moonen, B. D. Moor, L. Vandenberghe, and J. Vandewalle, “On- and off-line identification of linear state-space models,” *International Journal of Control*, vol. 49, no. 1, pp. 219–232, 1989.

[25] S. Geman, E. Bienenstock, and R. Doursat, “Neural networks and the bias/variance dilemma,” *Neural Computation*, vol. 4, no. 1, pp. 1–58, 1992.

[26] W. Favoreel, B. D. Moor, and M. Gevers, “SPC: Subspace predictive control,” *IFAC Proceedings Volumes*, vol. 32, no. 2, pp. 4004–4009, 1999.

[27] S. Sedghizadeh and S. Beheshti, “Data-driven subspace predictive control: Stability and horizon tuning,” *Journal of the Franklin Institute*, vol. 355, no. 15, pp. 7509–7547, 2018.

[28] I. Markovsky, J. C. Willems, P. Rapisarda, and B. L. D. Moor, “Data driven simulation with application to system identification,” in *16th IFAC World Congress*, vol. 38, no. 1. Elsevier BV, 2005, pp. 970–975.

[29] G. Q. Carapia, I. Markovsky, R. Pintelon, P. Z. Csurcsia, and D. Verbeke, “Experimental validation of a data-driven step input estimation method for dynamic measurements,” *IEEE Transactions on Instrumentation and Measurement*, vol. 69, no. 7, pp. 4843–4851, 2020.

[30] H. J. van Waarde, M. K. Camlibel, and M. Mesbahi, “From noisy data to feedback controllers: non-conservative design via a matrix S-lemma,” *arXiv preprint arXiv:2006.00870*, 2020.

[31] J. C. Willems and J. W. Polderman, *Introduction to mathematical systems theory: a behavioral approach*. Springer, 1997, vol. 26.

[32] I. Markovsky and S. V. Huffel, “Overview of total least-squares methods,” *Signal Processing*, vol. 87, no. 10, pp. 2283–2302, 2007.

[33] P. T. Boggs and J. W. Tolle, “Sequential quadratic programming,” *Acta numerica*, vol. 4, no. 1, pp. 1–51, 1995.

[34] A. Damen, P. Van den Hof, and A. Hajdasinski, “Approximate realization based upon an alternative to the Hankel matrix: the Page matrix,” *Systems & Control Letters*, vol. 2, no. 4, pp. 202–208, 1982.

[35] I. Markovsky and F. Dörfler, “Identifiability in the behavioral setting,” 2020, submitted for publication. Available: <http://homepages.vub.ac.be/~imarkovs/publications/identifiability.pdf>.

[36] G. Pilonetto and G. D. Nicolao, “A new kernel-based approach for linear system identification,” *Automatica*, vol. 46, no. 1, pp. 81–93, 2010.

- [37] T. Chen, "On kernel design for regularized LTI system identification," *Automatica*, vol. 90, pp. 109–122, 2018.
- [38] T. Chen, H. Ohlsson, and L. Ljung, "On the estimation of transfer functions, regularizations and gaussian processes—revisited," *Automatica*, vol. 48, no. 8, pp. 1525–1535, 2012.
- [39] R. Hallouzi and M. Verhaegen, "Fault-tolerant subspace predictive control applied to a Boeing 747 model," *Journal of Guidance, Control, and Dynamics*, vol. 31, no. 4, pp. 873–883, 2008.
- [40] R. Kadali, B. Huang, and A. Rossiter, "A data driven subspace approach to predictive controller design," *Control Engineering Practice*, vol. 11, no. 3, pp. 261–278, 2003.